TEV GAMMA-RAY OBSERVATIONS OF THE BINARY NEUTRON STAR MERGER GW170817 WITH H.E.S.S.

(H.E.S.S. Collaboration)[*]

H. Abdalla,[1] A. Abramowski,[2] F. Aharonian,[3,4,5] F. Ait Benkhali,[3] E.O. Angüner,[6] M. Arakawa,[7]
M. Arrieta,[8] P. Aubert,[9] M. Backes,[10] A. Balzer,[11] M. Barnard,[1] Y. Becherini,[12] J. Becker Tjus,[13]
D. Berge,[14] S. Bernhard,[15] K. Bernlöhr,[3] R. Blackwell,[16] M. Böttcher,[1] C. Boisson,[8] J. Bolmont,[17]
S. Bonnefoy,[18] P. Bordas,[3] J. Bregeon,[19] F. Brun,[20] P. Brun,[21] M. Bryan,[11] M. Büchele,[22] T. Bulik,[23]
M. Capasso,[24] S. Caroff,[25] A. Carosi,[9] S. Casanova,[6,3] M. Cerruti,[17] N. Chakraborty,[3] R.C.G. Chaves,[19,†]
A. Chen,[26] J. Chevalier,[9] S. Colafrancesco,[26] B. Condon,[20] J. Conrad,[27,‡] I.D. Davids,[10] J. Decock,[21]
C. Deil,[3] J. Devin,[19] P. deWilt,[16] L. Dirson,[2] A. Djannati-Ataï,[28] A. Donath,[3] L.O'C. Drury,[4] K. Dutson,[29]
J. Dyks,[30] T. Edwards,[3] K. Egberts,[31] G. Emery,[17] J.-P. Ernenwein,[32] S. Eschbach,[22] C. Farnier,[27,12]
S. Fegan,[25] M.V. Fernandes,[2] A. Fiasson,[9] G. Fontaine,[25] S. Funk,[22] M. Füssling,[18,*] S. Gabici,[28]
Y.A. Gallant,[19] T. Garrigoux,[1] F. Gaté,[9] G. Giavitto,[18] B. Giebels,[25] D. Glawion,[33] J.F. Glicenstein,[21]
D. Gottschall,[24] M.-H. Grondin,[20] J. Hahn,[3] M. Haupt,[18] J. Hawkes,[16] G. Heinzelmann,[2] G. Henri,[34]
G. Hermann,[3] J.A. Hinton,[3] W. Hofmann,[3] C. Hoischen,[31,*] T. L. Holch,[35] M. Holler,[15] D. Horns,[2]
A. Ivascenko,[1] H. Iwasaki,[7] A. Jacholkowska,[17] M. Jamrozy,[36] D. Jankowsky,[22] F. Jankowski,[33] M. Jingo,[26]
L. Jouvin,[28] I. Jung-Richardt,[22] M.A. Kastendieck,[2] K. Katarzyński,[37] M. Katsuragawa,[38] U. Katz,[22]
D. Kerszberg,[17] D. Khangulyan,[7] B. Khélifi,[28] J. King,[3] S. Klepser,[18] D. Klochkov,[24] W. Kluźniak,[30]
Nu. Komin,[26] K. Kosack,[21] S. Krakau,[13] M. Kraus,[22] P.P. Krüger,[1] H. Laffon,[20] G. Lamanna,[9] J. Lau,[16]
J.-P. Lees,[9] J. Lefaucheur,[8] A. Lemière,[28] M. Lemoine-Goumard,[20] J.-P. Lenain,[17] E. Leser,[31] T. Lohse,[35]
M. Lorentz,[21] R. Liu,[3] R. López-Coto,[3] I. Lypova,[18] D. Malyshev,[24] V. Marandon,[3] A. Marcowith,[19]
C. Mariaud,[25] R. Marx,[3] G. Maurin,[9] N. Maxted,[16,§] M. Mayer,[35] P.J. Meintjes,[39] M. Meyer,[27,¶]
A.M.W. Mitchell,[3] R. Moderski,[30] M. Mohamed,[33] L. Mohrmann,[22] K. Morå,[27] K. Morå,[27] E. Moulin,[21]
T. Murach,[18] S. Nakashima,[38] M. de Naurois,[25] H. Ndiyavala,[1] F. Niederwanger,[15] J. Niemiec,[6] L. Oakes,[35]
P. O'Brien,[29] H. Odaka,[38] S. Ohm,[18,*] M. Ostrowski,[36] I. Oya,[18] M. Padovani,[19] M. Panter,[3] R.D. Parsons,[3]
N.W. Pekeur,[1] G. Pelletier,[34] C. Perennes,[17] P.-O. Petrucci,[34] B. Peyaud,[21] Q. Piel,[9] S. Pita,[28]
V. Poireau,[9] H. Poon,[3] D. Prokhorov,[12] H. Prokoph,[14] G. Pühlhofer,[24] M. Punch,[28,12] A. Quirrenbach,[33]
S. Raab,[22] R. Rauth,[15] A. Reimer,[15] O. Reimer,[15] M. Renaud,[19] R. de los Reyes,[3] F. Rieger,[3,**]
L. Rinchiuso,[21] C. Romoli,[4] G. Rowell,[16] B. Rudak,[30] C.B. Rulten,[8] V. Sahakian,[40,5] S. Saito,[7]
D.A. Sanchez,[9] A. Santangelo,[24] M. Sasaki,[22] R. Schlickeiser,[13] F. Schüssler,[21,*] A. Schulz,[18]
U. Schwanke,[35] S. Schwemmer,[33] M. Seglar-Arroyo,[21,*] M. Settimo,[17] A.S. Seyffert,[1] N. Shafi,[26] I. Shilon,[22]
K. Shiningayamwe,[10] R. Simoni,[11] H. Sol,[8] F. Spanier,[1] M. Spir-Jacob,[28] Ł. Stawarz,[36] R. Steenkamp,[10]
C. Stegmann,[31,18] C. Steppa,[31] I. Sushch,[1] T. Takahashi,[38] J.-P. Tavernet,[17] T. Tavernier,[28] A.M. Taylor,[18]
R. Terrier,[28] L. Tibaldo,[3] D. Tiziani,[22] M. Tluczykont,[2] C. Trichard,[32] M. Tsirou,[19] N. Tsuji,[7] R. Tuffs,[3]
Y. Uchiyama,[7] D.J. van der Walt,[1] C. van Eldik,[22] C. van Rensburg,[1] B. van Soelen,[39] G. Vasileiadis,[19]
J. Veh,[22] C. Venter,[1] A. Viana,[3,††] P. Vincent,[17] J. Vink,[11] F. Voisin,[16] H.J. Völk,[3] T. Vuillaume,[9]
Z. Wadiasingh,[1] S.J. Wagner,[33] P. Wagner,[35] R.M. Wagner,[27] R. White,[3] A. Wierzcholska,[6] P. Willmann,[22]
A. Wörnlein,[22] D. Wouters,[21] R. Yang,[3] D. Zaborov,[25] M. Zacharias,[1] R. Zanin,[3] A.A. Zdziarski,[30] A. Zech,[8]
F. Zefi,[25] A. Ziegler,[22] J. Zorn,[3] and N. Żywucka[36]

[1] Centre for Space Research, North-West University, Potchefstroom 2520, South Africa

[2] Universität Hamburg, Institut für Experimentalphysik, Luruper Chaussee 149, D 22761 Hamburg, Germany

[3] Max-Planck-Institut für Kernphysik, P.O. Box 103980, D 69029 Heidelberg, Germany

[4] Dublin Institute for Advanced Studies, 31 Fitzwilliam Place, Dublin 2, Ireland

[5] National Academy of Sciences of the Republic of Armenia, Marshall Baghramian Avenue, 24, 0019 Yerevan, Republic of Armenia

[6] Instytut Fizyki Jądrowej PAN, ul. Radzikowskiego 152, 31-342 Kraków, Poland

[7] Department of Physics, Rikkyo University, 3-34-1 Nishi-Ikebukuro, Toshima-ku, Tokyo 171-8501, Japan

[8] LUTH, Observatoire de Paris, PSL Research University, CNRS, Université Paris Diderot, 5 Place Jules Janssen, 92190 Meudon, France

contact.hess@hess-experiment.eu

[9] *Laboratoire d'Annecy-le-Vieux de Physique des Particules, Université Savoie Mont-Blanc, CNRS/IN2P3, F-74941 Annecy-le-Vieux, France*

[10] *University of Namibia, Department of Physics, Private Bag 13301, Windhoek, Namibia*

[11] *GRAPPA, Anton Pannekoek Institute for Astronomy, University of Amsterdam, Science Park 904, 1098 XH Amsterdam, The Netherlands*

[12] *Department of Physics and Electrical Engineering, Linnaeus University, 351 95 Växjö, Sweden*

[13] *Institut für Theoretische Physik, Lehrstuhl IV: Weltraum und Astrophysik, Ruhr-Universität Bochum, D 44780 Bochum, Germany*

[14] *GRAPPA, Anton Pannekoek Institute for Astronomy and Institute of High-Energy Physics, University of Amsterdam, Science Park 904, 1098 XH Amsterdam, The Netherlands*

[15] *Institut für Astro- und Teilchenphysik, Leopold-Franzens-Universität Innsbruck, A-6020 Innsbruck, Austria*

[16] *School of Physical Sciences, University of Adelaide, Adelaide 5005, Australia*

[17] *Sorbonne Universités, UPMC Université Paris 06, Université Paris Diderot, Sorbonne Paris Cité, CNRS, Laboratoire de Physique Nucléaire et de Hautes Energies (LPNHE), 4 place Jussieu, F-75252, Paris Cedex 5, France*

[18] *DESY, D-15738 Zeuthen, Germany*

[19] *Laboratoire Univers et Particules de Montpellier, Université Montpellier, CNRS/IN2P3, CC 72, Place Eugène Bataillon, F-34095 Montpellier Cedex 5, France*

[20] *Université Bordeaux, CNRS/IN2P3, Centre d'Études Nucléaires de Bordeaux Gradignan, 33175 Gradignan, France*

[21] *IRFU, CEA, Université Paris-Saclay, F-91191 Gif-sur-Yvette, France*

[22] *Friedrich-Alexander-Universität Erlangen-Nürnberg, Erlangen Centre for Astroparticle Physics, Erwin-Rommel-Str. 1, D 91058 Erlangen, Germany*

[23] *Astronomical Observatory, The University of Warsaw, Al. Ujazdowskie 4, 00-478 Warsaw, Poland*

[24] *Institut für Astronomie und Astrophysik, Universität Tübingen, Sand 1, D 72076 Tübingen, Germany*

[25] *Laboratoire Leprince-Ringuet, Ecole Polytechnique, CNRS/IN2P3, F-91128 Palaiseau, France*

[26] *School of Physics, University of the Witwatersrand, 1 Jan Smuts Avenue, Braamfontein, Johannesburg, 2050 South Africa*

[27] *Oskar Klein Centre, Department of Physics, Stockholm University, Albanova University Center, SE-10691 Stockholm, Sweden*

[28] *APC, AstroParticule et Cosmologie, Université Paris Diderot, CNRS/IN2P3, CEA/Irfu, Observatoire de Paris, Sorbonne Paris Cité, 10, rue Alice Domon et Léonie Duquet, 75205 Paris Cedex 13, France*

[29] *Department of Physics and Astronomy, The University of Leicester, University Road, Leicester, LE1 7RH, United Kingdom*

[30] *Nicolaus Copernicus Astronomical Center, Polish Academy of Sciences, ul. Bartycka 18, 00-716 Warsaw, Poland*

[31] *Institut für Physik und Astronomie, Universität Potsdam, Karl-Liebknecht-Strasse 24/25, D 14476 Potsdam, Germany*

[32] *Aix Marseille Université, CNRS/IN2P3, CPPM, Marseille, France*

[33] *Landessternwarte, Universität Heidelberg, Königstuhl, D 69117 Heidelberg, Germany*

[34] *Univ. Grenoble Alpes, CNRS, IPAG, F-38000 Grenoble, France*

[35] *Institut für Physik, Humboldt-Universität zu Berlin, Newtonstr. 15, D 12489 Berlin, Germany*

[36] *Obserwatorium Astronomiczne, Uniwersytet Jagielloński, ul. Orla 171, 30-244 Kraków, Poland*

[37] *Centre for Astronomy, Faculty of Physics, Astronomy and Informatics, Nicolaus Copernicus University, Grudziadzka 5, 87-100 Torun, Poland*

[38] *Japan Aerpspace Exploration Agency (JAXA), Institute of Space and Astronautical Science (ISAS), 3-1-1 Yoshinodai, Chuo-ku, Sagamihara, Kanagawa 229-8510, Japan*

[39] *Department of Physics, University of the Free State, PO Box 339, Bloemfontein 9300, South Africa*

[40] *Yerevan Physics Institute, 2 Alikhanian Brothers St., 375036 Yerevan, Armenia*

ABSTRACT

We search for high-energy gamma-ray emission from the binary neutron star merger GW170817 with the H.E.S.S. Imaging Air Cherenkov Telescopes. The observations presented here have been obtained starting only 5.3h after GW170817. The H.E.S.S. target selection identified regions of high probability to find a counterpart of the gravitational wave event. The first of these regions contained the counterpart SSS17a that has been identified in the optical range several hours after our observations. We can therefore present the first data obtained by a ground-based pointing instrument on this object. A subsequent monitoring campaign with the H.E.S.S. telescopes extended over several days, covering timescales from 0.22 to 5.2 days and energy ranges between 270 GeV to 8.55 TeV. No significant

gamma-ray emission has been found. The derived upper limits on the very-high-energy gamma-ray flux for the first time constrain non-thermal, high-energy emission following the merger of a confirmed binary neutron star system.

[*] corresponding author (contact.hess@hess-experiment.eu)

[†] Funded by EU FP7 Marie Curie, grant agreement No. PIEF-GA-2012-332350

[‡] Wallenberg Academy Fellow

[§] Now at The School of Physics, The University of New South Wales, Sydney, 2052, Australia

[¶] Now at Kavli Institute for Particle Astrophysics and Cosmology, Department of Physics and SLAC National Accelerator Laboratory, Stanford University, Stanford, California 94305, USA

[**] Heisenberg Fellow (DFG), ITA Universität Heidelberg, Germany

[††] Now at Instituto de Física de São Carlos, Universidade de São Paulo, Av. Trabalhador São-carlense, 400 - CEP 13566-590, São Carlos, SP, Brazil

1. INTRODUCTION

Opening the era of gravitational wave (GW) astronomy, the first direct detection of a GW signal from a binary black hole merger was reported by the LIGO-Virgo scientific collaboration (LVC) on September 2015 (Abbott, B.P. et al. (LVC) 2016) during the first science run (O1) of the Advanced LIGO interferometers. The second science run O2 started in fall 2016 with the two LIGO detectors taking data. The Advanced Virgo interferometer joined the observations on August 1, 2017. Marking the beginning of gravitational wave multimessenger astronomy, a gravitational wave signal compatible with that expected from the merger of a binary neutron star system was detected by the LIGO-Virgo collaboration on August 17, 2017 (Abbott, B.P. et al. (LVC) 2017). The event stands as the first direct detection of gravitational waves coming from a system of this kind. As these events are assumed to be related to Gamma-Ray Bursts (GRBs) or kilonovae (Metzger & Berger 2012), broadband emission of electromagnetic (EM) radiation as well as high-energy neutrinos (Eichler et al. 1989) can be expected in addition to the gravitational wave signal. An extensive observational campaign covering a very wide range of EM wavelengths from radio to high-energy gamma rays and including high-energy neutrinos was launched immediately after the detection of the GW signal.

Gamma-Ray Bursts are short bursts of radiation with prompt emission typically detected in the tens of keV to GeV range (e.g. Zhang et al. 2006). The duration of the initial, or prompt, emission follows a bimodal distribution, with the divisional timescale between both types of bursts being around 2 seconds (Kouveliotou et al. 1993). This distinction enables their classification into *short* GRB (sGRB) and *long* GRB (lGRB). These classes have been linked to the association of the events with different cosmic progenitors. The long GRBs are usually associated with the core-collapse of massive stars (Woosley et al. 2007; Piran et al. 2017), while the coalescence of a compact binary system, being either a neutron star-neutron star (NS-NS) or a neutron star-black hole, are thought to be the cosmic progenitors of short GRBs that have a hard spectrum (Piran 1994; Metzger & Berger 2012). In these systems, the orbit of the binary system steadily decays as a result of the energy loss through continuous gravitational wave emission, resulting in the objects spiraling inwards at an increasing rate. At the final phase of the process, a characteristic burst of gravitation radiation is emitted, a prime signal for current GW instruments. In addition, the GW radiation is expected to be accompanied by both thermal and non-thermal emission in the form of EM radiation. Depending on the mass losses during the cataclysmic event, the residual compact object left afterwards will be a black hole or a neutron star. However, due to strong absorption at early times and the beaming effects associated with relativistic outflows of the post-merger ejecta, the EM radiation from the inner engine may be shrouded from view. Therefore, a gravitational wave observation of such an event, provides substantial new information to characterize the progenitor system and the phenomena leading to the explosive merger.

One of the leading theoretical frameworks describing the phenomenology of GRBs is the so-called fireball model (Meszaros & Rees 1993; Piran 1999). After the formation of a new compact object, the central engine releases a huge amount of energy over a short time and within a small volume, giving rise to relativistic outflows and shocks. This *fireball* is considered to consist of an optically thick electron-positron/photon plasma expanding with relativistic velocities.

Additionally, another class of EM transient counterpart to mergers of binary neutron stars has been proposed. These events are called *Macronovae* (Kulkarni 2005) or *Kilonovae* (Metzger et al. 2010), and their energy output lies between the novae and supernovae energy scales. Kilonovae produce delayed optical, UV and infrared radiation on timescales of a few days, heated by the radioactive decay of r-process elements in the ejecta itself, or in the interaction of the ejecta with the interstellar medium (see e.g. Tanvir et al. 2013, for a GRB-Kilonova association). The ejecta in a kilonova are believed to have a mass of $\sim 10^{-2} M_{\odot}$ and are moving at mildly-relativistic velocities of 0.1-0.2c. Kilonovae produce rather isotropic emission that typically lasts for days after the merger event (see Baiotti & Rezzolla 2017, and references therein).

Clear evidence for a non-thermal emission from sGRBs has been found in the GeV energy range for only a handful of cases (Ackermann et al. 2013a), with maximum observed photon energies exceeding 30 GeV (Ackermann et al. 2010). In principle, this gamma-ray emission may be produced via energy losses from particles accelerated at shocks present in the outflow or formed when the ejecta propagate through the interstellar medium. Given the ejected mass and ejecta velocities considered, this situation is reminiscent of a supernova remnant where diffusive shock acceleration would proceed in the non-relativistic to trans-relativistic regime (Ellison et al. 2013). With its superior sensitivity on short timescales above 50 GeV, relative to the Fermi-LAT instrument, the High Energy Stereoscopic System (H.E.S.S. II) is uniquely suited to probe the level of non-thermal emission produced by high energy

transient events (Hoischen, C. et al. (H.E.S.S. Collaboration) 2017).

High energy observations of non-thermal emission in the GeV-TeV energy range thus provide an effective probe of non-thermal emission from both *fireball* and *kilonovae* classes of events. With the significant sensitivity achieved in this energy range, a detection of a cut-off in the spectral energy distribution of the emission is possible, which would provide hints on the environment of the cataclysmic event (Ackermann et al. 2011) and allow one to estimate the kinematic velocities of the outflow in which the γ-ray emission was produced. Moreover, the comparison between the highest and the low-energy photons from the same source can provide constraints on theories of Lorentz invariance violation (Biesiada & Piórkowska 2009).

This article is organized as follows. In Sec. 2, the gravitational wave event, the subsequent EM follow-up campaign and the H.E.S.S. follow-up effort is discussed. Section 3 describes the data and their analysis and in Section 4 the results are described. Discussion and conclusion are presented in Section 5.

2. NEUTRON STAR MERGER FOLLOW-UP

2.1. *Electromagnetic follow-up of GW alerts*

In preparation of the physics data taking of the advanced LIGO and Virgo interferometers, agreements with an extensive group of observatories interested in performing follow-up observations across the EM spectrum and using high-energy neutrinos has been set up by the LIGO-Virgo collaboration. H.E.S.S. became a member of this group in early 2015 and the follow-up of gravitational wave alerts has been prepared (see Sec. 2.3.1 for details).

To rapidly alert the MWL follow-up community, the LIGO-Virgo collaboration has developed different low-latency pipelines searching for transient signals from compact binary mergers. The fastest pipeline is BAYESTAR (Singer & Price 2016). It is complemented by the LALInference, which is scanning a larger parameter space and marginalizing over calibration uncertainties and is thus providing a more robust estimate of the important event parameters (Veitch et al. 2015).

2.2. *GW170817*

A gravitational wave event was recorded on August 17, 2017, at 12:41:04 UTC by the Advanced LIGO and Advanced Virgo interferometers (Abbott, B.P. et al. (LVC) 2017). Based on a BAYESTARS analysis using the data of the LIGO-Hanford instrument an initial alert reporting a highly significant detection of a binary neutron star

signal was issued to a wide range of follow-up observatories about 40 minutes after the event (The LIGO Scientific Collaboration and the Virgo Collaboration GCN Circ. 21505). As only data from a single interferometer was used in this initial reconstruction, the sky location of the event could only be localized to within $24,200 \deg^2$ (90% containment). Nevertheless the timing of the alert allowed the team of *Fermi* Gamma-Ray Burst Monitor (Fermi-GBM) to correlate the GW event with a gamma-ray burst (170817A, V. Connaughton et al. (Fermi-GBM Collaboration) GCN Circ. 21506; von Kienlin et al. (Fermi-GBM Collaboration) GCN Circ. 21520) observed $\sim 1.7\,$s after the gravitational-wave candidate. The light-curve of the GRB event shows a weak short pulse with a duration of 2 seconds, typical for *short* GRBs (Goldstein, A. et al. (Fermi-GBM Collaboration) GCN Circ. 21528). GRB170817A has also been recorded by the SPI-ACS instrument onboard the Integral satellite (Savchenko et al. (Integral) 2017). Further details are given in Abbott, B.P. et al. (Fermi-GBM, Integral, LVC) (2017).

On Aug 17, 2017, at 17:54:51 UTC, the LIGO-Virgo collaboration provided an update on the gravitational wave skymap, incorporating data from the LIGO Livingston detector (which had to be excluded in the initial analysis due to a noise artifact) as well as data from the Virgo detector in the BAYESTAR pipeline (The LIGO Scientific Collaboration and the Virgo Collaboration GCN Circ. 21513, BAYESTAR_HLV in the following). The result of this joint analysis reduced the 90% localization uncertainty of the GW event to about $31 \deg^2$. The data confirmed the binary neutron star origin and located the merger event at a distance of $40 \pm 8\,$Mpc ($50 \pm 3\,$Mpc if assuming the binary to be face on). A further analysis using the LALInference method was provided about six hours later (The LIGO Scientific Collaboration and the Virgo Collaboration GCN Circ. 21527, 2017 Aug 17, 23:54:40 UTC). The 90% credible region of this map (cf. Fig. 2) spans $34 \deg^2$, overlapping with the 90 % uncertainty region of GRB170817A (Goldstein, A. et al. (Fermi-GBM Collaboration) 2017). The final estimates of the source properties of GW170817 are given in Abbott, B.P. et al. (LVC) (2017).

The first EM counterpart to GW170817 and GRB170817A was detected in the near-infrared by the One-Meter Two-Hemisphere (1M2H) collaboration with the 1 m Swope telescope at Las Campanas Observatory in Chile on Aug 17 at 23:33 UTC, i.e. 10.87 hr after GW170817 (Coulter et al. (1M2H Collaboration) 2017). The source, located at $\alpha(J2000.0) = 13^{h}09^{m}48^{s}.085 \pm 0.018$, $\delta(J2000.0) = -23°22'53''.343 \pm 0.218$, near the early-type galaxy NGC 4993 at a distance of 42.5 Mpc, got designated Swope
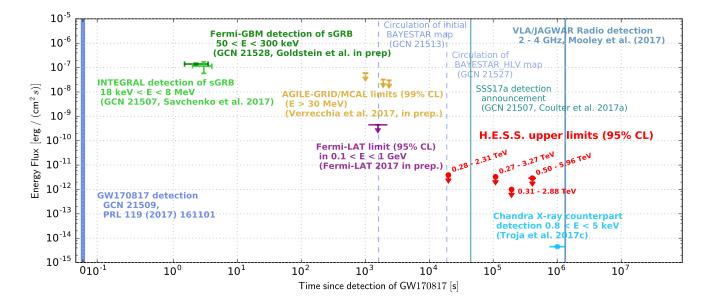
Figure 1. Timeline of the observations following the detection of GW170817 with a focus on the high-energy, non-thermal domain. A more complete picture of the multi-wavelength and multi-messenger campaign is given in (Abbott, B.P. et al. (LVC and EM follow-up group) 2017).

Supernova Survey 2017a (SSS17a). It had an initial brightness of magnitude 17.3 ± 0.1 in the i band (Coulter et al. (1M2H Collaboration) GCN Circ. 21567). The IAU designation of the source is AT2017gfo. NGC 4993 is on the list of possible candidates that had been identified by "Global Relay of Observatories Watching Transients Happen" network (Cook et al. (GROWTH Collaboration) GCN Circ. 21519) via cross-matching the gravitational wave localization with the "census of the local universe" catalogue (Cook et al. 2016). The optical transient was detected independently by five different teams: the Distance Less Than 40Mpc (DLT40) survey (Yang et al.), by Tanvir et al. (VISTA), Lipunov et al. (MASTER), Allam et al. (DECam) and Arcavi et al. (Las Cumbres Observatory). Archival searches (e.g. ASAS-SN (Cowperthwaite et al. GCN Circ. 21533), Hubble (Foley et al. GCN Circ. 21536), etc.) did not show evidence of emission at this position in observations taken before the GW event.

The subsequent MWL follow-up campaign focused mainly on the optical transient SSS17a. The monitoring of the source in the UV, optical and near-infrared domain allows the detailed description of its spectral evolution over timescales extending from hours to several days and weeks. The source has also been monitored in UV and X-rays by Swift (Evans et al. (Swift) 2017) over several days. An X-ray source coincident with the location of SSS17a has been discovered by Chandra about 9 days after GW170817 (Troya et al. (Chandra) 2017). In the radio domain, the first counterpart con-

sistent with the optical transient position was identified September 2 and 3, 2017, (16 days after GW170817) by two observations using the Jansky VLA (Mooley et al. (JVLA/JAGWAR) GCN Circ. 21814; Corsi et al. (VLA) GCN Circ. 21815).

This extensive monitoring campaign covering the full EM spectrum, including the high-energy (HE) and very-high-energy (VHE) gamma ray domains (the latter reported in this paper) and searches for high-energy neutrinos, allowed us to monitor the evolution of the source over several days. Focusing on the high-energy, non-thermal domain, a subset of the observations obtained during this campaign is shown in Fig. 1. Further details of this unprecedented multi-wavelength and multi-messenger effort can be found in (Abbott, B.P. et al. (LVC and EM follow-up group) 2017) and references therein.

2.3. H.E.S.S. follow-up of GW170817

Here we report on observations obtained in the very-high energy gamma-ray domain with the H.E.S.S. imaging atmospheric Cherenkov telescope array. H.E.S.S. is located on the Khomas Highland plateau of Namibia ($23°16'18''$ South, $16°30'00''$ East), at an elevation of 1800 m above sea level. With its original four-telescope array, H.E.S.S. is sensitive to cosmic and gamma-rays in the 100 GeV to 100 TeV energy range and is capable of detecting a Crab-like source close to zenith and under good observational conditions at the 5σ level within less than one minute (Aharonian et al. 2006). In 2012

a fifth telescope with 28 m diameter was commissioned, extending the covered energy range toward lower energies. The observations reported here were conducted jointly with three of the original 12 m telescopes and the 28 m telescope. One of the 12 m H.E.S.S. telescopes was not available due to a maintenance campaign.

2.3.1. *Scheduling for GW follow-up*

The localization uncertainty derived from the data of the GW interferometers is significant for events detected by two interferometers (hundreds to thousands of square degrees) and still sizable for events with data from three detectors (tens to hundreds of square degrees). Although the field-of-view of the large 28 m H.E.S.S. telescope and the four 12 m telescopes has a radius of about 1.5 deg and 2.5 deg, respectively, several pointings are typically necessary to cover the identified region. An additional challenge is related to the limited duty-cycle of the observatory, operating only in astronomical darkness during moonless nights and the accessible range of zenith angles (usually < 60 deg). Since H.E.S.S. joined the EM follow-up group of the LIGO-Virgo collaboration, several algorithms have been developed to optimize the follow-up of GW events while taking into account these constrains. The most straightforward and most general scheduling algorithms determine the pointing of the telescopes by maximizing the coverage of the two-dimensional localization probability provided with the GW alerts. In addition to these algorithms, we developed optimized strategies for events occurring at distances for which sufficient complete galaxy catalogs are available. For these we use the GLADE catalogue (Dalya et al. 2016), a value-added full-sky galaxy catalog highly complete and specifically built in order to support EM follow-up of GW signals. It includes more than 3 million entries and is (outside the Galactic plane) complete up to ~ 70 Mpc, well matching the horizon of the current GW interferometers to detect mergers of binary neutron star systems.

Our approach follows the one outlined by Singer et al. (2016). We use the full three-dimensional information of the location of the GW-event provided by the BAYESTAR and LALInference GW pipelines and correlate it with the location of galaxies within that volume. Several algorithms have been implemented to derive an optimized pointing scenario from this 3D GW-Galaxies probability region. The *One-in-FoV* algorithm searches for the coordinates that provide the highest probability of hosting the event, while the *Gal-in-FoV* algorithm determines the center of a region on the sky which provides best coverage of neighboring high-probability regions falling in the same field-of-view. Both algorithms

are taking into account observational constraints like the available time window and, trying to achieve a low energy threshold, optimize the pointing strategy favoring low-zenith angle observations. Both are complementary in terms of calculation speed and performance, with *One-in-FoV* being used for real-time follow-ups and the *Gal-in-FoV* for offline scheduling. Further details about the developed approaches and performance estimates based on Monte Carlo simulations of NS-NS merger events are given in Seglar-Arroyo, M., Schüssler, F. (H.E.S.S. Collaboration) (2017).

2.3.2. *Scheduling for GW170817*

As outlined above, the first localization map for the event GW170817 was provided by the BAYESTAR pipeline and was made available to follow-up partners about 1.5 h after the GW event (The LIGO Scientific Collaboration and the Virgo Collaboration GCN Circ. 21509). Due to its large uncertainty covering $24,200$ deg^2 at 90% containment, it was not suitable for scheduling follow-up observations. An updated BAYESTAR-reconstructed GW map, BAYESTAR_HLV, using data from all three interferometers was received about 5 hours after the event, at 17:54 UTC (The LIGO Scientific Collaboration and the Virgo Collaboration GCN Circ. 21513). This map, with the 90% region of the localization uncertainty covering 31 deg^2, was used for the scheduling of H.E.S.S. follow-up observations. With H.E.S.S. data taking starting on August 17 at 17:59 UTC, only about 5 minutes were available to derive a pointing strategy. A LAL-Inference based sky map was made available about 9 hours after the gravitational wave event. Changes with respect to the low-latency BAYESTAR_HLV map were minimal (the 90% uncertainty region increased slightly to 34 deg^2).

Due to the limited time between the publication of the BAYESTAR_HLV map and the start of the visibility window we used the *One-in-FoV* approach to determine the H.E.S.S. pointing schedule for the night of Aug 17/18. Three observation runs of 28 min each were scheduled. They are given in Tab. 1 and illustrated in Fig. 2. The three observations were taken between Aug 17, 17:59 - 19:30 UTC. For an effective FoV of 1.5 deg radius of the H.E.S.S. 28 m telescope, they cover about 56 % of the gravitational wave uncertainty region of the final LALInference map. At the same time they include about 86% of the probability density region obtained by weighting the three-dimensional GW map with galaxies from the GLADE catalog. All three pointings are compatible with GRB1707A within 2σ. Whereas the optical transient SSS17a had not been discovered at the
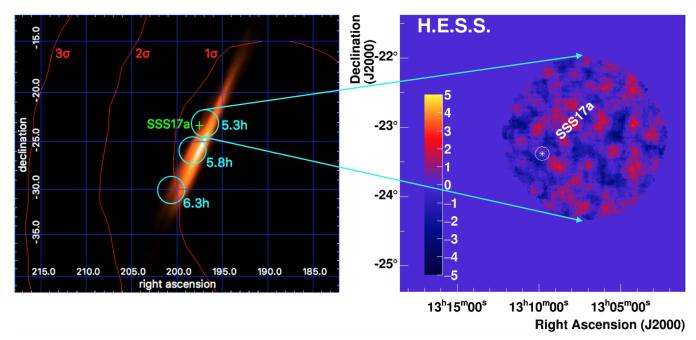
Figure 2. Left: Pointing directions of the first night of H.E.S.S. follow-up observations starting August 17, 2017, at 17:59 UTC. The circles illustrate a FoV with radius of 1.5 deg and the shown times are the starting times of each observation with respect to GW170817. The LALInference map of GW170817 is shown as colored background, the red lines denote the uncertainty contours of GRB170817A. Right: Map of significances of the gamma-ray emission in the region around SSS17a obtained during the first observation of GW170817. The white circle has a diameter of 0.1deg, corresponding to the H.E.S.S. point spread function and also used for the oversampling of the map.

time our observations took place, the focus on a region containing many galaxies compatible with the 3D-GW map allowed us to cover NGC 4993 and SSS17a with our first observation, i.e. starting 5.3h after the GW event. We note that our observations have the shortest time delay with respect to GW170817 by any ground-based pointing instrument participating in the follow-up of GW170817.

After the detection of SSS17a during the night of Aug 17/18 we discontinued further coverage of the GW uncertainty region and focussed on monitoring the source in TeV gamma-rays. H.E.S.S. observations were scheduled at the beginning of the following nights around SSS17a as long as the location was visible from the H.E.S.S. site within a maximum zenith angle of about 60 deg and fulfilling the necessary observation conditions. The obtained observations are summarized in Table 1.
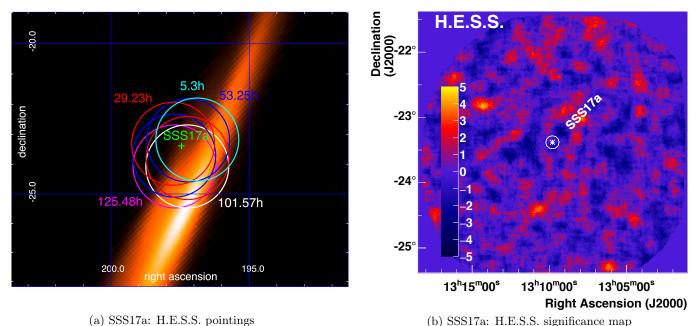
3. DATA AND ANALYSIS

The obtained data were analyzed using Model Analysis (de Naurois & Rolland 2009), an advanced Cherenkov image reconstruction method in which the recorded shower images are compared to a semi-analytical model of gamma ray showers by means of a log-likelihood optimization. We perform our analysis using only data from the 28 m telescope in the center of the H.E.S.S.

Table 1. H.E.S.S. follow-up observations of GW170817. All pointings were taken with the default run duration of 28 min and are given in equatorial J2000 coordinates.

ID	Observation time (UTC)	Pointing coordinates [deg]	$<$zenith angle$>$ [deg]
1a	2017-08-17 17:59	196.88, -23.17	59
1b	2017-08-17 18:27	198.19, -25.98	58
1c	2017-08-17 18:56	200.57, -30.15	62
2a	2017-08-18 17:55	197.75, -23.31	53
2b	2017-08-18 18:24	197.23, -23.79	60
3a	2017-08-19 17:56	197.21, -23.20	55
3b	2017-08-19 18:24	197.71, -23.71	60
5a	2017-08-21 18:15	197.24, -24.07	60
6a	2017-08-22 18:10	197.70, -24.38	60

array in order to achieve a low energy threshold. The "Loose cuts" of Model Analysis were adopted. These cuts require, among other criteria, the total charge in the shower image to be greater than 60 photoelectrons. The resulting energy threshold, defined as the energy where the acceptance is 10% of its maximum value, is about 280 GeV for the first observation and 270 GeV for the combined dataset on SSS17a. The threshold is sig-

(a) SSS17a: H.E.S.S. pointings

(b) SSS17a: H.E.S.S. significance map

Figure 3. Left plot: H.E.S.S. pointing directions during the monitoring campaign of SSS17a. For details see Tab. 1. The circles denote a FoV with radius of 1.5 deg and the shown times are the start times of each observation with respect to GW170817. Right plot: Map of significances of the gamma-ray emission in the region around SSS17a combining all observations obtained during the H.E.S.S. monitoring campaign.

nificantly influenced by the relatively high zenith angle of the observations. The background level in the FoV was determined from the dataset itself using the standard "ring background" technique (Berge et al. 2007), a robust method ideally suited to derive gamma-ray emission maps in FoVs with low number of sources. In order to derive the acceptance function required as input to the ring background method, we exploited the azimuthal symmetry of the acceptance across the field-of-view of the telescopes. We require that at least 10 events are available for the background estimation, a requirement that limits the energy range over which our results are valid. The derived energy ranges are given in Tab. 2. Further analyses exploiting the data from the full H.E.S.S. array will be published at a later time.

The results of the data analysis have been verified with an independent analysis relying on a fully independent data calibration chain and using the Image Pixel-wise fit for Atmospheric Cherenkov Telescopes (ImPACT, Parsons & Hinton 2014) reconstruction method. The results from this cross-check analysis are consistent with the ones presented here, thus providing confidence in the robustness of the presented results.

While propagating through the extragalactic radiation fields, high-energy gamma rays interact with the extragalactic background light (EBL) via e^+/e^- pair-creation processes. This leads to the collective effect of an absorption of gamma-rays at the highest energies. The resulting gamma-ray opacity depends on the energy as well

as on the distance of the source. Using the EBL model published in Franceschini, A. et al. (2008) we are able to calculate energy dependent EBL correction factors. Using the redshift of NGC4993, $z = 0.009787$ (Wenger et al. 2000), these factors increase with energy and are about 10 % (30 %) at 1 TeV (10 TeV). These effects are therefore only of minor importance and we here do not correct for them in this paper.

The region covered by our observations contains several sources with emission in the GeV energy range. They are for example listed in the catalog compiled after four-year long observations by the LAT instrument onboard the Fermi satellite (Acero et al. 2015). None of them is known to exhibit emission in the TeV range [1]. The most promising TeV candidate source in the region is likely PKS 1309-216, at an angular distance of 1.58 deg from NGC4993/SSS17a. It has a flux in the $1 - 100$ GeV range of about 2.0×10^{-11} erg cm^{-2} s-1 and an energy spectrum following $E^{2.07\pm0.05}$ in the same energy range. Extrapolating the emission to the higher energies relevant for our observations needs to account for EBL absorption effects: at the redshift of PKS 1309-216 ($z = 1.489$ (Wenger et al. 2000)) the initial flux is decreased by more than one order of magnitude at energies around 100 GeV and by a factor exceeding 10^9 at 1 TeV (Franceschini, A. et al. 2008). Conservatively,

---

[1] http://tevcat.uchicago.edu

we nevertheless excluded a region with a 0.3 deg radius around PKS 1309-216 from the background estimation used for the analysis presented here.

None of the GeV detected sources showed significant flux increases during the period of the observations presented here (Ackermann et al. 2013b). We therefore conclude that no TeV gamma-ray emission exceeding the level of the reached sensitivity, other than a potential signal related to GW170817 and GRB170817A, is expected.

We note that archival H.E.S.S. observations on PKS 1309-216 have been obtained in 2013. After about 10 h of observations, neither gamma-ray emission from the source nor from the region around NGC 4993 / SSS17a could be detected. We therefore derive an archival upper limit on the gamma-ray flux at from SSS17a from these observations to $\Phi(170\,\mathrm{GeV} < E < 47.2\,\mathrm{TeV}) < 3.1 \times 10^{-12}\,\mathrm{erg\,cm^{-2}\,s^{-1}}$ at 95 % C.L. and assuming a spectral index of -2. The differential upper limit as function of energy is shown in the left plot of Fig. 4.

4. RESULTS

As outlined above, our observations of SSS17a started August 17, 2017, at 17:59 UTC (pointing 1a) and were repeated during several nights (cf. Tab. 1). The different pointings, except 1b and 1c, which are not covering SSS17a but were taken during the initial scanning of the GW170817 uncertainty region, are shown in the left plot of Fig. 3. The same color is used for pointings obtained successively during the same night and the numbers indicate the time difference between the start of the observations and the time of GW170817. As the potential gamma-ray emission from a NS-NS merger is expected to be transient, we analyzed each of the obtained nightly datasets independently. For each of them we produce skymaps of the gamma-ray excess counts above the background derived from the data itself as described above. These excess maps have then been converted into significance maps using the formalism described by Li & Ma (1983).

As example, we show the gamma-ray significance map derived from the first observation in Fig. 2. An oversampling radius of 0.1 deg, roughly corresponding to the H.E.S.S. point-spread function has been applied. No significant gamma-ray emission is found within any of the individual datasets and all of the obtained results are fully compatible with the background-only expectation. We thus conclude that no significant gamma-ray afterglow was detected from the direction of SSS17a. Consequently we derive 95 % C.L. upper limits on the gamma-ray flux following Feldman & Cousins (1998). The obtained flux limits, assuming a generic E^{-2} en-

ergy spectrum for the potential emission, are given together with the corresponding energy ranges in Tab. 2 and shown in Fig. 1.

Table 2. Limits on the high-energy gamma-ray flux at 95 % C.L. and assuming a E^{-2} energy spectrum obtained during the monitoring of SSS17a with H.E.S.S.
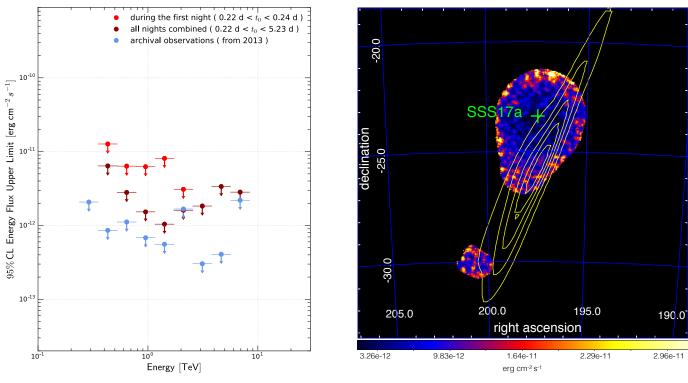
pointings (see Tab.1)	time since GW trigger [days]	f_γ [erg cm^{-2} s^{-1}]	Energy band [TeV]
1a	0.22	$< 3.9 \times 10^{-12}$	0.28–2.31
2a+2b	1.22	$< 3.3 \times 10^{-12}$	0.27–3.27
3a+3b	2.22	$< 1.0 \times 10^{-12}$	0.31–2.88
5a+6a	4.23, 5.23	$< 2.9 \times 10^{-12}$	0.50–5.96
all	0.22 – 5.23	$< 1.5 \times 10^{-12}$	0.27–8.55

In a search for fainter but temporally extended emission from SSS17a, we combined all datasets (except 1b and 1c). The obtained significance map (cf. right plot of Fig. 3) is again fully compatible with the background-only hypothesis. We obtain $\Phi_\gamma < 1.5 \times 10^{-12}\,\mathrm{erg\,cm^{-2}\,s^{-1}}$ in the energy band $0.27 < E[\mathrm{TeV}] < 8.55$. Assuming a radially symmetric emission this flux limit corresponds to a limit on the gamma-ray luminosity of SSS17a at a distance of 42.5 Mpc of $L_\gamma < 3.2 \times 10^{41}\,\mathrm{erg\,s^{-1}}$. We note the luminosity of the prompt phase of GRB170817A that has been found to be around $2.2 \times 10^{46}\,\mathrm{erg\,s^{-1}}$ by Integral SPI-ACS (Savchenko et al. (Integral) 2017). Differential upper limits as function of the energy are shown in the left plot of Fig. 4 for the first observation on SSS17a, the combined dataset and the archival observations obtained in 2013.

After combining all observations obtained with H.E.S.S. during the follow-up campaign of GW170817 we derive a sky map showing the integral upper limits in the 270 GeV to 8.55 TeV energy range. It is shown in the right plot of Fig. 4. First of all it illustrates the deep observations centered on SSS17a. Induced by the radially decreasing acceptance of the telescope, the obtained limits are less constraining when approaching the border of the field-of-view. The figure also illustrates the achieved $\approx 50\%$ coverage of the LALInference map of GW170817, which is depicted by the yellow contours.

5. DISCUSSION AND CONCLUSION

The observations presented here represent the first very-high-energy gamma-ray observations following the merger of a binary neutron star system. A prepre-

(a) SSS17a: H.E.S.S. limits

(b) GW170817: H.E.S.S. flux limit map

Figure 4. Left plot: Differential upper limits on the gamma-ray flux from SSS17a derived from the H.E.S.S monitoring campaign and archival observations of the region. Right plot: Map showing the integral upper limits in the 270 GeV to 8.55 TeV energy range (assuming an E^{-2} energy spectrum) derived from the H.E.S.S. follow-up observations of GW170817. The yellow contours outline the localization of the GW event as provided by the LALInference map.

pared scheduling procedure which allowed fast reaction to the event and its optimization which provided efficient pointing within the gravitational wave uncertainty region, succeeded in covering observational fields including that of the multi-wavelength counterpart SSS17a, even before it had been discovered from optical observations. Following the discovery of this counterpart in the optical band, subsequent extended monitoring allowed deep observations to be made of this source. Although the source was not detected within the energy range $0.27 < E[\text{TeV}] < 8.55$, the derived upper limits are the most stringent ones obtained on hour to week-long timescales, of non-thermal emission from GW170817 in the full gamma-ray domain ranging from keV to TeV energies. They allow for the first time a constraint to be placed on the level of early-time very-high-energy emission from the source, following the binary neutron star merger. With a potential connection to a *kilonova* type event, expected to give rise to the ejection of mildly relativistic outflows, further observations of this object should be performed to probe particle acceleration beyond TeV energies on longer timescales.

12

REFERENCES

Abbott, B.P. et al. (Fermi-GBM, Integral, LVC). 2017, ApJL in press, doi:10.3847/2041-8213/aa920c

Abbott, B.P. et al. (LVC). 2016, Phys. Rev. Lett., 116, 061102

—. 2017, Phys. Rev. Lett., 119, 161101

Abbott, B.P. et al. (LVC and EM follow-up group). 2017, ApJL in press, doi:10.3847/2041-8213/aa91c9

Acero, F., Ackermann, M., Ajello, M., et al. 2015, ApJ, 218, 23

Ackermann, M., Asano, K., Atwood, W. B., et al. 2010, ApJ, 716, 1178

Ackermann, M., Ajello, M., Asano, K., et al. 2011, ApJ, 729, 114

Ackermann, M., Ajello, M., Asano, K., et al. 2013a, ApJS, 209, 11

Ackermann, M., Ajello, M., Albert, A., et al. 2013b, ApJ, 771, 57

Aharonian, F., Akhperjanian, A. G., Bazer-Bachi, A. R., et al. 2006, A&A, 457, 899

Allam et al. (DECam). GCN Circ. 21530, 2017-08-18

Arcavi et al. (Las Cumbres Observatory). GCN Circ. 21538, 2017-08-18

Baiotti, L., & Rezzolla, L. 2017, Reports on Progress in Physics, 80, 096901

Berge, D., Funk, S., & Hinton, J. 2007, A&A, 466, 1219

Biesiada, M., & Piórkowska, A. 2009, Classical and Quantum Gravity, 26, 125007

Cook, D. O., Kasliwal, M. M., et al. 2016, in Proc. AAS Meeting, Vol. 227

Cook et al. (GROWTH Collaboration). GCN Circ. 21519, 2017-08-17

Corsi et al. (VLA). GCN Circ. 21815, 2017-09-04

Coulter et al. (1M2H Collaboration). 2017, GCN Circ. 21529 and in prep.

—. GCN Circ. 21567, 2017-08-18

Cowperthwaite, P. S., Foley, R. J., & Berger, E. GCN Circ. 21533, 2017-08-18

Dalya, G., Frei, Z., Galgoczi, G., Raffai, P., & de Souza, R. 2016, VizieR Online Data Catalog, 7275

de Naurois, M., & Rolland, L. 2009, Astropart. Physics, 32, 231

Eichler, D., Livio, M., Piran, T., & Schramm, D. N. 1989, Nature, 340, 126

Ellison, D. C., Warren, D. C., & Bykov, A. M. 2013, ApJ, 776, 46

Evans et al. (Swift). 2017, GCN Circ. 21550 and Science submitted

Feldman, G. J., & Cousins, R. D. 1998, Physical Review D, 57, 3873

Foley, R. J., Kilpatrick, C. D., Nicholl, M., & Berger, E. GCN Circ. 21536, 2017-08-18

Franceschini, A. et al. 2008, A&A, 487, 837

Goldstein, A. et al. (Fermi-GBM Collaboration) . GCN Circ. 21528, 2017-08-18

Goldstein, A. et al. (Fermi-GBM Collaboration). 2017, ApJL, 848, doi:10.3847/2041-8213/aa8f4

Hoischen, C. et al. (H.E.S.S. Collaboration). 2017, Proc. 35th ICRC, arXiv:1708.01088

Kouveliotou, C., Meegan, C. A., Fishman, G. J., et al. 1993, ApJ, 413, L101

Kulkarni, S. R. 2005, ArXiv Astrophysics e-prints, astro-ph/0510256

Li, T.-P., & Ma, Y.-Q. 1983, ApJ, 272, 317

Lipunov et al. (MASTER). GCN Circ. 21546, 2017-08-18

Meszaros, P., & Rees, M. 1993, ApJ, 405, 278

Metzger, B. D., & Berger, E. 2012, ApJ, 746, 48

Metzger, B. D., Martínez-Pinedo, G., Darbha, S., et al. 2010, MNRAS, 406, 2650

Mooley et al. (JVLA/JAGWAR). GCN Circ. 21814, 2017-09-04

Parsons, R. D., & Hinton, J. A. 2014, Astropart. Physics, 56, 26

Piran, T. 1994, AIP Conference Proceedings, 307, 543

—. 1999, Physics Reports, 314, 575

Piran, T., Nakar, E., Mazzali, P., & Pian, E. 2017, arXiv preprint arXiv:1704.08298

Savchenko et al. (Integral). 2017, GCN Circ. 21507 and APJL submitted

Seglar-Arroyo, M., Schüssler, F. (H.E.S.S. Collaboration). 2017, Rencontres de Moriond VHEPU (2017), arXiv:1705.10138

Singer, L. P., & Price, L. R. 2016, Physical Review D, 93, 024013

Singer, L. P., Chen, H.-Y., Holz, D. E., et al. 2016, ApJL, 829, L15

Tanvir, N. R., Levan, A. J., Fruchter, A. S., et al. 2013, Nature, 500, 547

Tanvir et al. (VISTA). GCN Circ. 21576, 2017-08-18

The LIGO Scientific Collaboration and the Virgo Collaboration. GCN Circ. 21505, 2017-08-17

—. GCN Circ. 21509, 2017-08-17

—. GCN Circ. 21513, 2017-08-17

—. GCN Circ. 21527, 2017-08-17

Troya et al. (Chandra). 2017, GCN Circ. 21765 and Nature in press

V. Connaughton et al. (Fermi-GBM Collaboration). GCN Circ. 21506, 2017-08-17

Veitch, J., Raymond, V., Farr, B., et al. 2015, Physical Review D, 91, 042003

von Kienlin et al. (Fermi-GBM Collaboration). GCN Circ. 21520, 2017-08-17

Wenger, M., Ochsenbein, F., Egret, D., et al. 2000, A&AS, 143, 9

Woosley, S., Blinnikov, S., & Heger, A. 2007, arXiv preprint arXiv:0710.3314

Yang, S., Valenti, S., Sand, D., Tartaglia, L., & Cappellaro, E. GCN Circ. 21531, 2017-08-18

Zhang, B., Fan, Y. Z., Dyks, J., et al. 2006, ApJ, 642, 354